

Actively-Induced Percolation: An Effective Approach to Multiple-Object Systems Characterization

Luciano da Fontoura Costa

*Institute of Physics of São Carlos. University of São Paulo,
São Carlos, SP, PO Box 369, 13560-970, phone +55 162 73 9858,
FAX +55 162 71 3616, Brazil, luciano@if.sc.usp.br*

(Dated: 10th April 2004)

The present work proposes the concept of induced percolation over multiple-object systems, so that features such as the number of merged clusters can be used as a relevant measurement. The suggested approach involves the expansion of the objects while monitoring the evolving clusters. The potential of the proposed methodology for characterizing the spatial interaction and distribution between several objects is illustrated with respect to synthetic and real data.

PACS numbers: 64.60.Cn, 64.60.-i, 64.60.Ak, 87.57.Nk

Great part of the current interest in statistical physics and complex systems targets critical phenomena, such as percolation [1]. Characterized by abrupt changes of the system properties as some parameter is varied, critical phenomena are of interest because of their rich and complex dynamics. As a matter of fact, while the calculation of critical exponents for continuous phase transitions has been identified as one of the greatest achievements of theoretical physics over the last 25 years [2], the study of geometric percolation in graphs has provided one of the main motivations of the new area of complex networks [3]. Much interest has been focused on the analysis, modeling and simulation of natural critical phenomena, whereas relatively little attention has been given to *artificially-induced critical phenomena*, namely the enforcement of the objects in the system to undergo some imposed dynamics — e.g. expansion or dilation — in terms of a control parameter, so that critical phenomena can be induced. Although the intrinsic relevance of such investigations is potentially limited by the imposed evolution dynamics, it is argued and illustrated in the current work that such experiments present great potential for the characterization of the spatial distribution of objects while taking into account their shape and topology. This perspective provides a novel approach to the old problem of geometric characterization of multiple-object physical systems, which has been approached from several perspectives including densities (e.g. [4, 5]), additive functionals (e.g. [6]), fractal dimension (e.g. [7, 11]) and lacunarity (e.g. [8]). The importance of obtaining an effective methodology for the characterization of the spatial distribution and interaction in such systems is greatly enhanced by the myriad of related physical and biological systems, including statistical physics, astrophysics, geology, material science and even genetics (e.g. the spatial patterns of gene expression [9]). Although the proposed methodology can be immediately extended to continuous spaces, the following developments are limited to discrete structures as these are naturally required by several computational implementations and applications. In this article we start by presenting the proposed induced-percolation concepts and methods and proceed

by validating and illustrating them with respect to uniform point densities, perturbed hexagonal lattices and real data regarding the spatial distribution of retinal ganglion cells (e.g. [5]).

Let Ω be the N -dimensional Euclidean space where the multiple-object system is embedded and S be the set containing the coordinates (x, y) of each point of each object, in any order. The definition of the subsets of points corresponding to each object can be done by considering the respective point connectivity or by imposing previous knowledge about their classes (in this case a single object may include more than one connected component). In this work, every pair of points a and b such that $|x_a - x_b| + |y_a - y_b| = 1$ is linked through an undirected edge, so that each object corresponds to a connected component (or cluster) in Ω . Let also $R \in \Omega$ be a set delimitating the region of Ω where the artificially-induced dynamics is allowed. The Euclidean D -ring of the objects in Ω is obtained by determining the set of points of R which are no further away than D from the set S [13]. Only the distance values d_i allowed in the orthogonal lattice, i.e. $d_i = \sqrt{x^2 + y^2}$ for some x, y belonging to Ω , are considered in order to obtain full precision in spatially discrete spaces [10]. Observe that the density of such possible distances tends to increase with the distance. The dilation of S by the distance d_i can now be defined as the set of points obtained by the union of the original object and the respective $D = d_i$ -ring. Figure 1 shows a multiple-object system (a), the dilation of such a system for distances up to $D = 10$ (b), which can also be understood in terms of the exact distance transform of the objects [10].

The percolation dynamics considered in the present work involves the dilation, up to a maximum distance d_M , of the objects by each subsequent exact distance d_i , a scheme henceforth called *exact dilations* [10]. The exact distance d_i , or its respective index i [14], can both be considered as percolation parameter. Two are the immediate consequences of such an enforced dilation procedure: (i) the area of the objects increases monotonically; and (ii) contacts between objects occur at specific distance values, inducing the respective merging of the involved

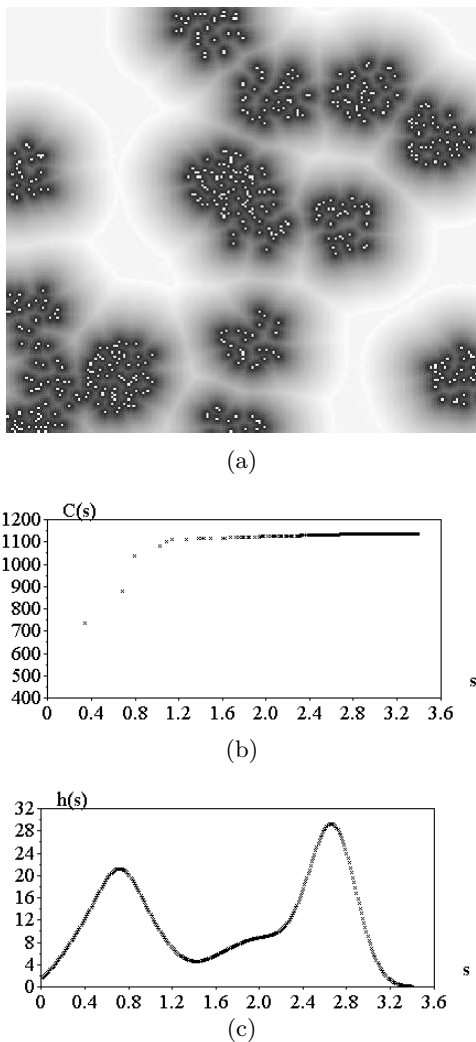


FIG. 1: The dilations of co-existing uniform particle densities (a) and the respective number of mergings $C(s)$ and $h(s)$ function.

clusters and possible critical phenomena. By associating each object to a node and incorporating edges between pairs of objects whenever they first touch one another, it is possible not only to merge the objects into larger clusters, but also to obtain the hierarchy induced by this agglomerative procedure.

Several measurements, such as the size of the maximum cluster [1, 3], could be considered in order to identify possible critical phenomena while the parameter i is increased, but the current work focuses on the cumulative number of clusters merged at each successive distances d_i , which is henceforth expressed as $C(d_i)$. We consider a square window with area A . In order to provide spatial-scale uniformity, we make the change of variable $C(k_i = \log(d_i))$. Now, considering uniform distribution of points (i.e. Poisson) with density γ as a reference model, the rate of change at k_j , while going from $C(k_j)$ to $C(k_{j+1})$, can be maximized by the finite difference

$q(k_j) = P(k_j)/\Delta k_j$, where $P(k_j) = \gamma A$ is the expected number of points inside R and $\Delta k_j = k_{j+1} - k_j$. In order to have the same change $q(k_i)$ for any value of k_i while considering uniform point densities inside the fixed window, we choose the changing rate at any specific value of k_j (in this article $j = 1$) as a reference and make the normalization as given in Equation 1. By adopting the minimal nearest neighbor distance as the prototype distance for the uniform distribution with density γ , we can use the mean expected value of such a distance, given as $d_i = \exp(k_i) = 1/(2\sqrt{\gamma})$ [11], in order to relate γ and k_i . By using this expression, we have that $P(k_i) = \gamma A = A/(4d_i^2)$ and $P(k_j) = A/(4d_j^2)$, so that $P(k_j)/P(k_i) = \exp(2k_i - 2k_j)$ and it is now possible to rewrite Equation 1 as Equation 2. Now, the derivative of the number of cluster mergings in terms of k_i for any type of point distribution can be approximated as in Equation 3, which is used henceforth. This equation already takes into account the fact that $k_{j=1} = 0$. An interpolated version of $w(k_i)$ can be obtained by first embedding it onto the continuous space s , such that $s = k_i$ at i , as expressed in Equation 4, and subsequently using the Parzen interpolating scheme [12] given in Equation 5 to obtain the function $h(s)$, where $g_\sigma(s) = 1/\sqrt{2\pi}/\sigma \exp(-0.5(s/\sigma)^2)$ is the normal density with standard deviation σ and ‘*’ stands for convolution. Figures 1(b) and (c) illustrates the distributions $C(s)$ and $h(s)$, respectively, for the multiple-object system in (a). The two co-existing Poisson densities in Figure 1(a), which were generated with $\gamma_1 = 0.05$ and $\gamma_2 = 0.002$, are clearly identified by the two peaks obtained in function $h(s)$. Each of these peaks have respective maximum value at $s_1 = 0.728$ and $s_2 = 2.673$, yielding estimated densities $\hat{\gamma}_1 = 1/(4 * \exp(2s_1)) = 0.058$ and $\hat{\gamma}_2 = 0.0012$. Considering the interferences between the two co-existing points distribution and the relatively poor sampling of the less dense distribution by the adopted 400×400 points window, such results can be considered as being reasonably accurate. Moreover, the fact that only a fraction of the denser distribution present in the window is duly expressed by the lower peak obtained for that case. Observe that such a multimodal distribution could by no means be obtained by using nearest-neighbor distance statistics.

$$Q(k_i) = \frac{P(k_i)}{\Delta k_i} \left(\frac{\Delta k_i P(k_j)}{\Delta k_j P(k_i)} \right) \quad (1)$$

$$Q(k_i) = \frac{P(k_i)}{\Delta k_j} \exp(2k_i - 2k_j) \quad (2)$$

$$w(k_i) = [C(k_{i+1}) - C(k_i)] / \Delta k_1 \exp(2k_i) \quad (3)$$

$$w(s) = \sum_{i=1}^M w(k_i) \delta(s - d_i) \quad (4)$$

$$h(s) = \sum_{i=1}^M [w(k_i) \delta(d_i)] * g_\sigma(s) \quad (5)$$

$$d(s) = 2\gamma\pi \exp(2s - \gamma\pi e^{2s}) \quad (6)$$

In order to further validate the proposed methodology, it has been applied to a series of uniform point distributions with increasing densities $\gamma = 1/(4d^2)$, where $d = 1, 2, \dots, 15$ are the characteristic spatial scales, estimated by nearest-neighbor distances. A 200×200 points window was adopted. The cases obtained for $d = 3, 7, 11$ and 15 are shown in Figure 2. Two interesting results have been identified: (i) a reasonably good estimation of the typical densities can be obtained by using the suggested methodology; and (ii) the functions $h(s)$ practically do not change their shape or heights for the different cases. It is also interesting to observe that the obtained functions are similar, but not identical, to the nearest-neighbor distributions given by Equation 6, also presented in Figure 2.

The potential of the proposed methodology for quantifying the degree of disorder [4] in point distributions was also evaluated by considering hexagonal lattices with increasing levels of uniformly distributed noise. More specifically, the basic hexagonal distribution was characterized by basic cells with sides of 10 points, with progressive perturbations added to the points coordinates. A 200×200 window was also considered for this case. It is clear from the obtained results that the perturbation degree is immediately reflected by the dispersion of the obtained functions $h(s)$, while the typical point density (indicated by the position of the peaks) is kept fixed. The sharpest peak is obtained for the noiseless hexagonal structure. The nearest-neighbor distributions for respective density is also shown (solid line) superposed to the $h(s)$, whose relatively narrow dispersion indicates that the point system is far from the disorder characteristic of uniform distributions.

In addition to the above validations performed with synthetic data, the proposed approach for characterization of multiple-object systems was also applied to real data regarding the spatial distribution of the center of mass of the soma of retinal ganglion cells, kindly provided by H. Wässle. Reflecting the hexagonal organization of the photoreceptors characterizing the central portion of the mammals' retina, the position of these cells at the last retinal layer are also expected to follow some hexagonal organization, with some degree of disorder. The obtained rings around each original point and the respective function $h(s)$ are shown in Figures 4(a) and (b), respectively. The nearest-neighbor distribution considering uniformly spaced points for the same density are also shown (solid

line) superposed to the curve $h(s)$ in Figure 4. It is clear from this result that the ganglion cell distribution is substantially narrower than its respective uniform counterpart, corroborating a more organized scheme such as the hexagonal spacing.

All in all, a new and effective approach to the characterization of multiple-object systems, based on artificially-induced percolation, has been proposed that presents a series of unique and interesting features. By considering only the exact distances representable in discrete spaces, as well as the fact that possibly co-existing point densities in such systems are typically sampled by using the same window, it has been possible to derive a powerful normalized tool capable not only of estimating the density of co-existing object distributions but also their respective perturbation degree. In addition, the number of points present in the observed region is reflected by the height of the obtained peaks. It is argued that such a function provides one of the most informative and accurate means for quantification of densities and spatial coverage, with the additional advantage that, unlike alternative schemes based on fractal and lacunarity, the obtained curve $h(s)$ has an immediate and intuitive interpretation in terms of point densities. Although not illustrated in this work, the proposed method can be immediately applied to multiple-object systems involving objects with shape and size more general than points. In such cases, the typical size of the objects has also been considered for the correct normalization and interpretation of the results. Other perspectives to be pursued further regard the consideration of the hierarchical structures (a tree) obtained as a byproduct of the percolation-induced merging procedure and the possibility of applying the artificially-induced percolation analysis to characterize weighted networks. The proposed approach is currently being applied to characterize the texture of bones, growing neural systems, and spatial patterns of gene expression.

Acknowledgments

The author is grateful to FAPESP (proc. 99/12NPq (proc. 301422/92-3) and the Human Frontier Science Program for financial support.

[1] D. Stauffer and A. Aharony, *Introduction to Percolation Theory* (Taylor and Francis, 1994).
 [2] J. J. B. A. J. Fisher, N. J. Dowrick, and M. E. J. Newman, *The Theory of Critical Phenomena* (Clarendon Press, London, 1992).
 [3] R. Albert and A. L. Barabási, *Rev. Mod. Phys.* **74**, 47 (2002).
 [4] J. M. Ziman, *Models of Disorder* (Cambridge University

Press, London, 1979).
 [5] H. Wässle and H. J. Riemann, *Proc. R. Soc. Lond. B. Biol. Sci.* **200**, 441 (1978).
 [6] K. Michelsen and H. de Raedt, *Physics Report* **347**, 461 (2001).
 [7] B. H. Kaye, *A Random Walk Through Fractal Dimensions* (John Wilhe and Sons, 1994).
 [8] J. P. Hovi, A. Aharony, D. Stauffer, and B. B. Mandel-

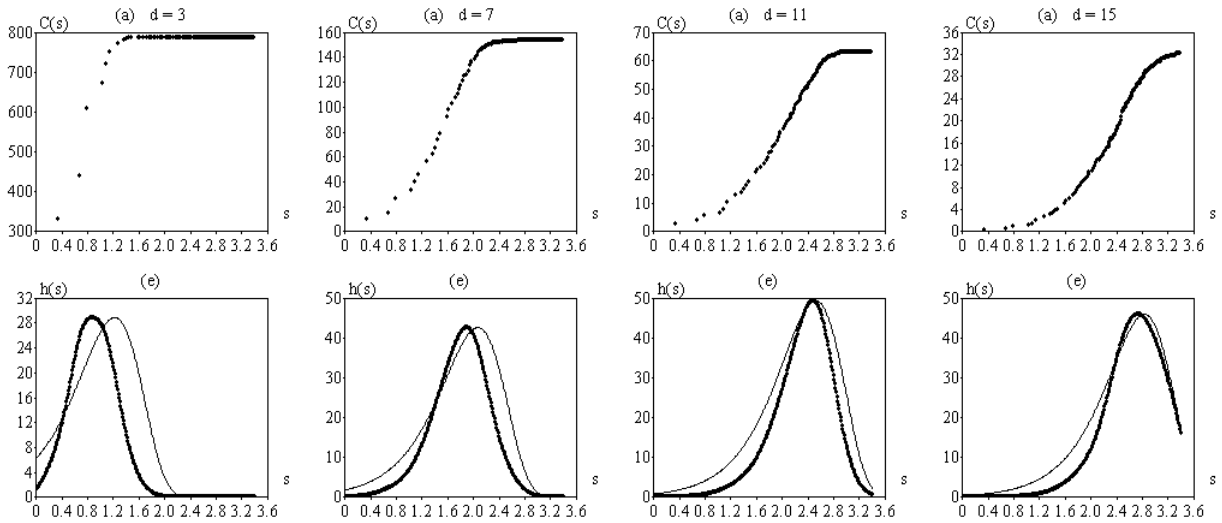


FIG. 2: Number of cluster mergings $C(s)$ (a-d) and respective $h(s)$ functions (e-h), represented by thick lines, obtained for uniform point densities with typical spatial scales 3, 7 11 and 15. The respective nearest-neighbor distributions are shown by the solid curves

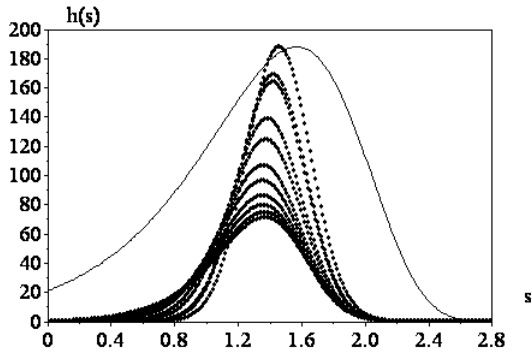
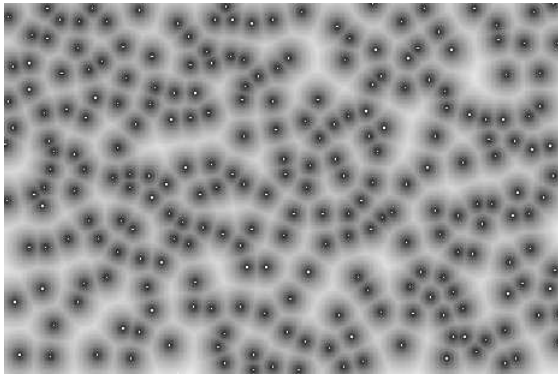
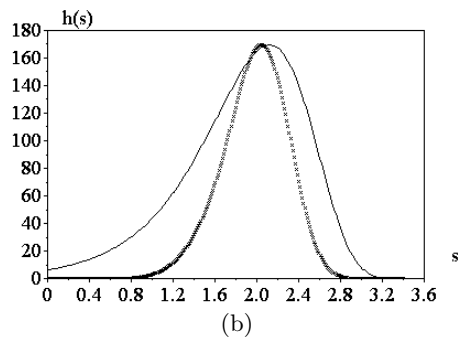


FIG. 3: Profiles of $h(s)$ (dotted lines) obtained for hexagonal point distributions with increasing levels of perturbation. The nearest-neighbor distribution obtained for uniform point dispersion with equivalent density is shown by the solid curve.

- brot, Phys. Rev. Lett. **77**, 877 (1996).
- [9] J. Streicher, M. A. Donat, B. Strauss, R. Spoerle, K. Schughart, and G. B. Muller, Nat. Genet. **25**, 147 (2000).
- [10] L. da F. Costa and R. M. C. Jr, *Shape Analysis and Classification: Theory and Practice* (CRC Press, Boca Raton, 2001).
- [11] D. Stoyan and H. Stoyan, *Fractals, Random Shapes and Point Fields* (John Wiley and Sons, Chichester, 1995).
- [12] R. O. Duda, P. E. Hart, and D. G. Stork, *Pattern Classification* (Wiley-Interscience, New York, 2001).
- [13] Recall that the distance between a point p and a set S of points corresponds to the minimal distance between p and any of the elements of S .
- [14] Observe that this index corresponds to the order of the exact distances d_i sorted in ascending order. For instance, in the case of the orthogonal lattices, we have $d_0 = 0$, $d_1 = 1$, $d_2 = \sqrt{2}$, etc.



(a)



(b)

FIG. 4: Spatial distribution of retinal ganglion cells (a) and respective $h(s)$ function (b), represented by the dotted line. The nearest-neighbor distribution obtained for uniform point dispersion with equivalent density is shown by the solid line.